Original article

The effective transfection of a low dose of negatively charged drug-loaded DNA-nanocarriers into cancer cells via scavenger receptors

Mirza Muhammad Faran Ashraf Baig [a, b, c, *], Chengfei Zhang [a],
Muhammad Furqan Akhtar [d], Ammara Saleem [e], Jahanzeb Mudassir [c]

[a] Laboratory of Biomedical & Pharmaceutical Engineering of Stem Cells Research, Restorative Dental Sciences, Faculty of Dentistry, The University of Hong Kong, 999077, Hong Kong, PR China
[b] State Key Laboratory of Analytical Chemistry for Life Sciences, School of Chemistry and Chemical Engineering, Nanjing University, Nanjing, 210023, PR China
[c] Faculty of Pharmacy, Bahauddin Zakariya University, Multan, 60000, Pakistan
[d] Riphah Institute of Pharmaceutical Sciences, Riphah International University, Lahore, Pakistan
[e] Department of Pharmacology, Faculty of Pharmaceutical Sciences, Government College University Faisalabad, Faisalabad, Pakistan

ARTICLE INFO

ABSTRACT

DNA-nanotechnology-based nano-architecture scaffolds based on circular strands were designed in the form of DNA-nanowires (DNA-NWs) as a polymer of DNA-triangles. Circularizing a scaffold strand (84-NT) was the critical step followed by annealing with various staple strands to make stiff DNA-triangles. Atomic force microcopy (AFM), native polyacrylamide gel electrophoresis (PAGE), UV-analysis, MTT-assay, flow cytometry, and confocal imaging were performed to assess the formulated DNA-NWs and cisplatin (CPT) loading. The AFM and confocal microscopy images revealed a uniform shape and size distribution of the DNA-NWs, with lengths ranging from 2 to 4 μm and diameters ranging from 150 to 300 nm. One sharp band at the top of the lane (500 bp level) with the loss of electrophoretic mobility during the PAGE (native) gel analysis revealed the successful fabrication of DNA-NWs. The loading efficiency of CPT ranged from 66.85% to 97.35%. MTT and flow cytometry results showed biocompatibility of the blank DNA-NWs even at 95% concentration compared with the CPT-loaded DNA-NWs. The CPT-loaded DNA-NWs exhibited enhanced apoptosis (22%) compared to the apoptosis (7%) induced by the blank DNA-NWs. The release of CPT from the DNA-NWs was sustained at < 75% for 6 h in the presence of serum, demonstrating suitability for systemic applications. The IC_{50} of CPT@DNA-NWs was reduced to 12.8 nM CPT, as compared with the free CPT solution exhibiting an IC_{50} of 51.2 nM. Confocal imaging revealed the targetability, surface binding, and slow internalization of the DNA-NWs in the scavenger-receptor-rich cancer cell line (HepG2) compared with the control cell line.

1. Introduction

The recently increased cancer prevalence among different age groups from pediatric to geriatric patients is devastating, requiring new tools to be developed for efficient treatment [1–4]. Cisplatin (CPT) is a drug of choice for chemotherapy of various types of cancers such as prostate, ovarian, cervical, testicular, brain, esophageal, liver, bladder, breast, lung, and head-neck cancers [3]. Being a hydrophilic drug, CPT presents a challenge in targeting tumor sites and is potentially cytotoxic to healthy cells. We have designed DNA-based nanocarriers (DNA-nanowires; (DNA-NWs)) to effectively load CPT (utilizing its DNA binding capability) and target cancer cells for intracellular CPT delivery [4]. We confirmed cancer cell targeting and intracellular delivery of CPT in a scavenger receptor-rich cell line (HepG2) as compared with the cell line that lacks scavenger receptors (CHSE-214 cell line) from the salamander embryo [5].

DNA nanotechnology is an effective approach for achieving nanoscale objects with the desired shape as carriers for drug

delivery and bio-imaging [6,7]. Watson/Crick base-pairing enables ease of self-assembly of various strands and the attainment of specific shapes. DNA binding drugs, including CPT, can be loaded effectively on compact DNA nano-architecture, owing to their intrinsic DNA-binding ability [8]. DNA-based nanomaterials are becoming increasingly crucial as drug delivery carriers due to their nanoscale size precision and control that can be exerted over the shape of the material [9,10]. Some drugs have the intrinsic ability to bind with the DNA double helix, such as doxorubicin and cisplatin, which can be effectively loaded onto DNA-based carriers [11,12].

Furthermore, the polyanionic nature of DNA renders internalization in healthy cells difficult [13]. As cancer cells have high proportions of polyanionic ligand-binding scavenger receptors, targeting cancer cells is more effective [14]. Triangular DNA tiles are synthesized after circularizing the template strand and annealing with staple strands [15,16]. Each triangle tile is designed to contain sticky ends at the vertices to combine (with each other), making a compact polymer, resulting in DNA-nanosheets that fold and spin onto itself due to the helical structure and curvature of the DNA to yield compact DNA-NWs [17,18]. After tagging CPT with the fluorescein isothiocyanate (FITC) dye, the loading of CPT/FITC onto the DNA-NWs was confirmed by confocal microscopy and UV analysis [19]. The mechanism of targeting and internalization of the CPT-loaded DNA-NWs is illustrated in Fig. 1.

2. Materials and methods

2.1. Chemicals and facilities

DNA-strands with the prescribed parameters and sequences were obtained from Sangon Biotechnology Company, Shanghai, China. Cisplatin (CPT; 99% purity) was purchased from Shanghai-Chemicals Company, Shanghai, China. MTT-reagent (3-(4,5-dimethylthiazol, 2 yl) 2,5-diphenyl-tetrazolium-bromide; 99% purity) was obtained from Sigma-Aldrich (St. Louis, MO, USA). HepG2 cells were provided by Nanjing University, Nanjing, China. Fast-Scan AFM by Bruker, USA was used for imaging and characterization of nanoparticles. Flow cytometry experiments were performed using a BD/LSR-FortessaX-20 flow cytometer (Becton-Dickinson, San Jose, CA, USA). Ninety-six-well plates were analyzed for UV−Vis measurements using a MultiScan-FC microplate-photometer by Thermo Fisher (Waltham, USA). The microliter volume samples were analyzed for UV−Vis measurements using a Thermo Fisher Nanodrop-2000c spectrometer (USA). Gel analysis was performed using a gel-apparatus by BioRad-Labs (CA, USA).

2.2. Preparation and characterization

The circular scaffold strands (84-NT) were annealed with staple strands to synthesize triangular DNA tiles. Triangular DNA tiles underwent cohesion polymerization via sticky ends at the vertices of the triangles to form DNA-NWs. The following are the detailed steps adopted for the preparation and characterization of DNA-NWs.

2.3. Triangular DNA-tiles and DNA-NWs

Specific DNA oligo sequences (Sangon-Biotech, Shanghai, China) were purified using the polyacrylamide gel electrophoresis (PAGE) method [20,21]. Purified oligos were UV-analyzed for concentration measurements using a Nanodrop-2000c. The ordered sequences of different DNA oligos are listed in Table 1. Schematics of the overall synthetic process are shown in Fig. 2.
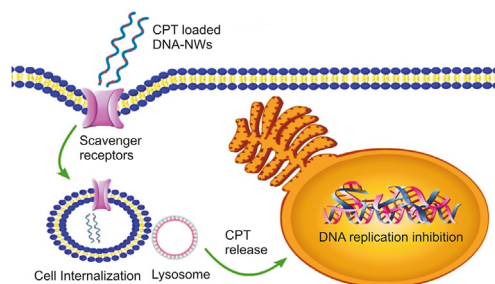
Fig. 1. Scavenger receptor-rich cancer cell line (HepG2) shows the rapid internalization of polyanionic DNA-nanocarriers for CPT delivery.

2.3.1. Preparing scaffold strands as a circularized template

Scaffold strands were circularized, as previously reported [22]. Briefly, a 5′-phosphorylated 50 μM linear scaffold (84-NT) was annealed with a 60 μM splint strand (20-NT) such that it was folded to join its two ends together with the help of splint strand [23]. The annealing process was performed from boiling to 25 °C over 3.5 h [24]. After joining the two ends of the scaffold strand with the help of splint strands, the two ends of the scaffold strand were covalently joined together via the ligation process using T4 DNA-ligase (8 μL, 350U/μL) at 16 °C for 16 h in the presence of freshly prepared TE buffer [25]. The ligating enzyme was heat-denatured, followed by exonuclease-1 treatment (8 μL, 5U/μL) for 35 min while incubating at 37 °C to digest and eliminate linear strands [22]. After that, exonuclease-1 was heat-denatured. After rapid re-cooling, 50 μL deionized form amide was added [26].

2.3.2. Purification of the circularized template

A denaturing-polyacrylamide gel (10%) was used to purify the freshly prepared circularized-template strand. The gel solution was made from a commercially available 3% acrylamide-bisacrylamide mixture in the presence of 4.0 M urea [27]. Electrophoresis was performed at 75 V for 4 h in TBE-EDTA buffer at 15 °C. The circularized template moved down the gel and gave a sharp band at the designated position under applied voltage and current [28,29]. The bands were cut corresponding to the circularized template and macerated in TE buffer at room temperature for 3 days using an orbital shaker to elute the gel's circularized template, followed by filtration using a syringe filtration assembly [20].

2.3.3. Synthesis of DNA triangles and CPT-loaded DNA-NWs

The circularized template strand was combined stoichiometrically with equimolar staple strands (30 μM) in the presence of TE buffer and 10% TAE-Mg buffer with the addition of 3 μL of the buffer per 30 μL of the final solution. A PCR machine (Thermo Fisher Scientific USA) was used for thermocycling the temperature with a gradual temperature drop from −1 °C to −0.1 °C every second to attain effective annealing without mismatch. As DNA triangular tiles contain sticky ends, they self-assemble in a robust way to make DNA 2D lattices in the form of sheets that coiled on its (own) axis to form DNA-NWs to act as a drug delivery carrier. FITC-tagged CPT was loaded onto the DNA-NWs using CPT's binding capability to double-stranded DNA [15].

2.4. Electrophoretic analysis of DNA triangle self-assembly to produce DNA-NWs

Assessing the restriction of the DNA's electrophoretic movement down the native-PAGE gel (a gel without urea) is a criterion for analyzing successful self-assembly of DNA triangular tiles into a large molecular-weight DNA lattice. Accordingly, the self-assembly

Table 1
Specific sequences of DNA oligos.

Name of DNA strand	Sequence (5'- 3')
Circular-template strand/84-NT	P-GACGGGCTAGGCCATATAACGTTAGGGATTCAGACTT GGAATCAACGTTCTGCCATGGACTCTTACTATGCATCGCCAGTACTC-
Staple-Strand 1/(34-NT)	GTCGACATGGCAGAACGTTGATTCCAAGTCTGAA
Staple-Strand 2/(40-NT)	GACCGCTGCCTAACGTTATATGGCCTAGCCCGTCCAGCTG
Staple-Strand 3/(34-NT)	GCGGTCGAGTACTGGCGATGCATAGTAAGAGTCC

of triangular DNA tiles was confirmed by native PAGE analysis using 10 μL of the annealed final assembly mixture of the large-sized DNA structure into the 10% PAGE gel to observe the restriction of the electrophoretic movement of the self-assembled DNA-NW samples into gel wells compared with other strands with different lengths and the DNA marker in the other wells of the gel as a control. The process was performed at a controlled temperature (10 °C) to avoid heating during the process under the TAE buffer. Different constituting DNA strands corresponding to the final self-assembly of DNA-NWs should not separate or segregate upon applied voltage and current (75 V, 20 A). This finding served as an indication of the integrity and strength of the self-assembly of DNA strands and the firm structure of the DNA-NW [17—19].

2.5. Procedure to assess CPT loading onto DNA-NWs

Since the absorption peak of the DNA and the CPT by UV light lies very close to each other (260—280 nm), accurate measurements could be doubtful. An alternative method for UV analysis was used to avoid this potential confound. CPT possesses amino groups in its chemical structure that can be conjugated to the conjugating dyes' carboxylic groups. Hook conjugating dye, manufactured by G-Biosciences (USA) and supplied by Sangon Biotechnology company (Shanghai, China), was successfully conjugated to the DNA-NWs using purification columns. The loading of the FITC-tagged CPT onto the DNA-NWs was determined through UV spectroscopy in relation to the absorption peak of FITC near 500 nm [30].

2.6. AFM to physically characterize DNA-NWs

A Bruker-FastScan AFM (Bruker Scientific, USA) was used for the analysis. A total of 5 μL of the final self-assembly (annealed) mixture was placed on the mica surface (freshly cleaved) to let DNA adhere to the mica surface for 5 min. It was followed by washing three times with the ultrapure water. Sample was air blown for drying to obtain a clean sample for AFM analysis. The imaging was performed by selecting three to four different locations, each of 5 μm × 5 μm areas to estimate the overall size, topology, surface characteristics, and size [31].
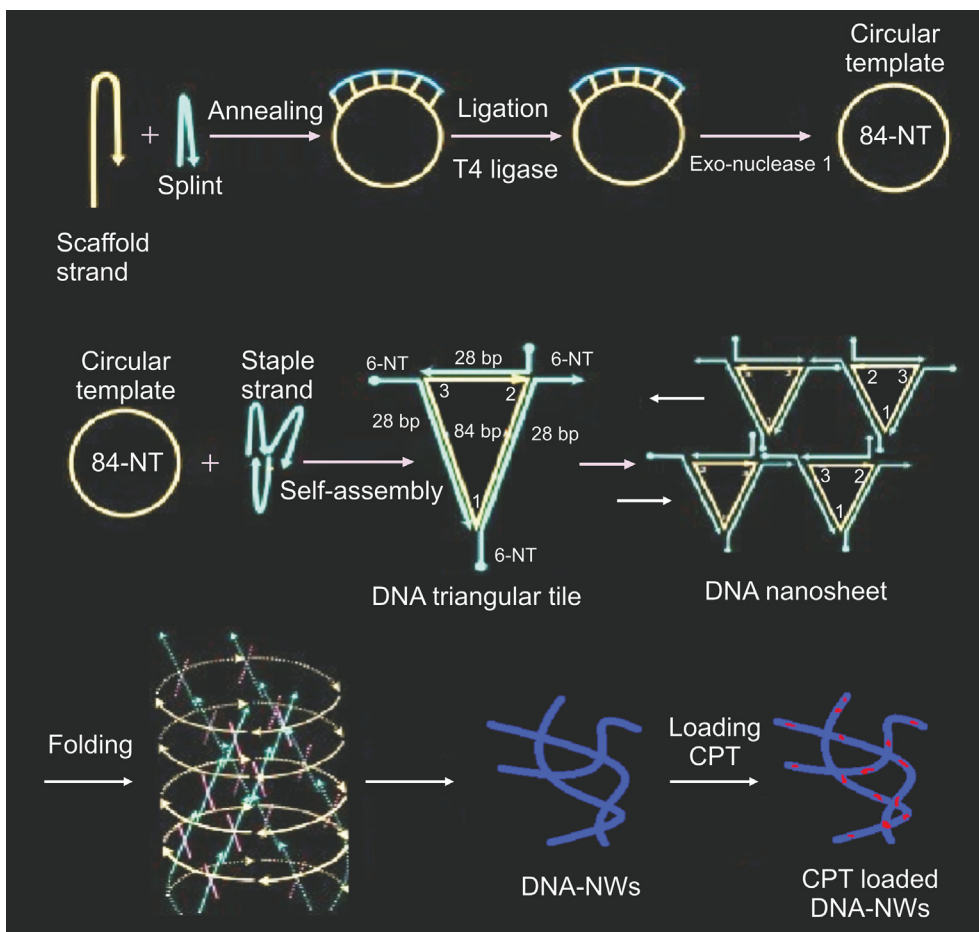
Fig. 2. A scheme to synthesize DNA-NW and FITC-tagged CPT loading.

2.7. Fluorescence imaging to characterize CPT loaded DNA-NWs

For fluorescence imaging of the DNA-NWs, we loaded FITC-tagged CPT on the DNA-NWs. We analyzed CPT loading under double photon confocal microscopy after making a glass slide [32].

2.8. The quantitative loading efficiency of CPT onto DNA-NWs

The mixture of CPT-loaded (FITC-tagged) DNA-NWs was incubated for 4 h, and then centrifuged at 14,000 rpm under reduced temperature and pressure to sediment the CPT-loaded DNA-NWs. The unbound CPT-FITC was estimated spectrophotometrically using a Nanodrop-2000c (Thermo Fisher Scientific, USA) from the supernatant mixture using Eq. (1) [22].

$$CPT\ loading\ (\%) = \frac{CPT_{total\ wt.}\ (\mu g) - CPT_{uloaded\ wt.}\ (\mu g)}{CPT_{total\ wt.}\ (\mu g)} \times 100 \tag{1}$$

2.9. Cell cultures

We used the HepG2 cell line (rich in scavenger receptors) for our targeting experiments and the CHSE-214 cell line (lacking scavenger receptors) from the salamander embryo as a control cell line. Low-glucose Dulbecco's modified-Eagle's medium (DMEM; Sangon-Biotechnology Company, Shanghai, China) was used for culturing HepG2 cells. In contrast, high-glucose DMEM (Sangon Biotechnology Company, Shanghai, China) with 10% fetal bovine serum (FBS) (Sangon-Biotechnology Company, Shanghai, China) and 100 U/mL antibiotic mixture (penicillin-streptomycin) was used for CHE-214 cells. Cells were cultured in 5% CO_2 and 37 °C in a humidified incubator (Thermo Fisher Scientific, USA).

2.10. Assessing cell viability, biocompatibility, and cytotoxicity using MTT analysis

2.10.1. Assessing the biocompatibility of the blank DNA-NW (without CPT loading)

To assess the biocompatibility of blank DNA-NW without CPT loading, we performed MTT-assays and flow cytometry experiments. HepG2 cells were cultivated at a cell density of 10,000 cells per well, using low-glucose with 10% FBS and antibiotics supplementation in a 96 well-plate under standard cell-culture conditions (37 °C, 5% CO_2) for a half day. Following the cultivation step, we prepared different concentrations of blank DNA-NWs and placed them into wells, followed by 36−48 h incubation [33]. The DNA-NW-treated adherent cells were washed twice with PBS after the removal of the growth medium. Cells were treated with 5mg/mL MTT reagent, followed by incubation for 3−4 h. The excess unreacted MTT was withdrawn, followed by the addition of 140−150µL DMSO to dissolve the crystalline product while incubating in the dark for 10−15 min. The plates were analyzed for UV absorption at 580−620 nm using a plate reader (Thermo Fisher Scientific, USA). Cell viability was analyzed using Eq. (2) [34].

2.10.2. Anti-cancer activity and cytotoxic analysis for the CPT-loaded DNA-NWs

The MTT assay was repeated to assess the cytotoxic potential of CPT-loaded DNA-NWs, keeping the same DNA-NW concentration as in the blank measurements with different CPT concentrations [34].

2.11. Flow cytometry assay for assessing cell proliferation and apoptosis

For the flow cytometry assay for assessing cell proliferation and apoptosis, HepG2 cells were grown in 6-well plates maintaining a cell density of approximately 1×10^6 cells/well at standard humidified cell-culture conditions (37 °C and 5% CO_2) for one day. The cultured cells were treated with the CPT loaded DNA-NWs (PI-tagged) for 48 h. The treatment group of cells were compared with the control group of cells receiving blank DNA-NWs (PI-tagged) without prior CPT loading. To make the single cell suspension, the adhered cells were detached by the trypsin treatment for 2 min at 37 °C. The pellets of the cells obtained through the centrifugation were washed with PBS twice. The washed cells were then re-suspended in the PBS. The sample was then subjected to a flow cytometry assay (Becton Dickinson, San-Jose CA, USA) for cell counting measurements using parameters set according to the PI dye fluorescence range [4].

2.12. Cell imaging using double-photon confocal laser microscopy

The FITC-tagged CPT was loaded onto the DNA-NWs. Two types of cell lines were selected. The HepG2 cell line was chosen to investigate scavenger receptor-mediated internalization of DNA-NWs and cancer cell killing after being treated with DNA-NW solution for 12 h. A control cell line (CHSE-214) from the salamander embryo that lacked scavenger receptors was used as a control, which was hypothesized to show no DNA-NW internalization for 12 h [35].

2.13. Statistical interpretations

All of the experiments were reproduced thrice to achieve statistical significance.

3. Results and discussion

3.1. Confirmation of successful self-assembly of the DNA triangles into DNA-NWs and CPT loading

After the polymerization of DNA-triangular tiles, the resulting giant DNA nanolattices were assessed by gel electrophoresis. Next, we observed the restricted electrophoretic movement of the polymerized DNA nanolattices down the native-PAGE gel (a gel without urea). This movement provides evidence for the successful self-assembly of DNA triangular tiles into a large molecular weight DNA lattice [36]. It also provides a clue about the strength and integrity of the resulting DNA lattices, as constituting strands should not segregate under the applied voltage and current down the gel. Therefore, native PAGE analysis gave us an initial clue about the self-assembly of triangular DNA tiles by observing the

$$Cell\ viability\ (\%) = \left[\frac{(control\ sample\ absorbance - treated\ sample\ absorbance)}{control\ sample\ absorbance} \right] \times 100 \tag{2}$$
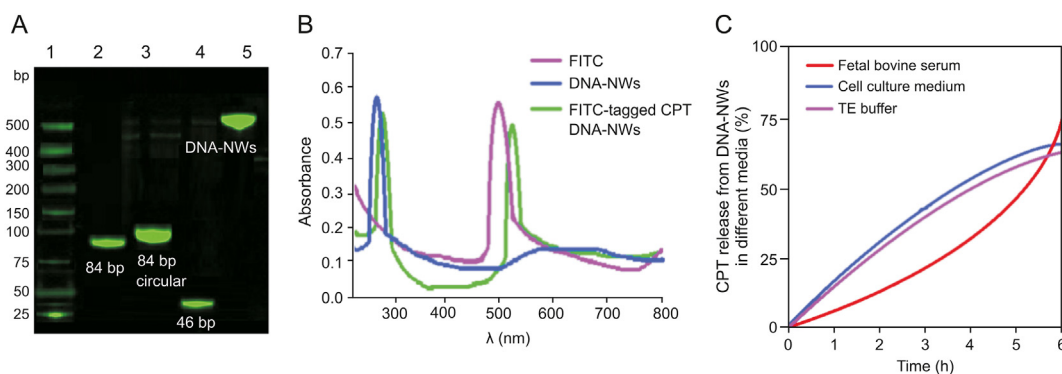
Fig. 3. (A) Electrophoretic analysis of the self-assembly of DNA triangles through native PAGE. (B) UV peak shift analysis to confirm CPT loading onto DNA-NWs. (C) Percentage of CPT release from the DNA-NWs in the different media.

restriction of the electrophoretic movement of the self-assembled DNA-NW samples down the gel (Lane 5) compared to other short monomeric strands with different lengths (Lanes 2 to 4), and strands in the DNA marker (Lane 1) moving down the gel to the greater distances [20], as shown in Fig. 3A.

The shifts confirmed the loading of CPT onto DNA-NWs in the UV peaks of the DNA (260−300 nm), CPT (280 nm), and the FITC dye (500−520 nm) that was tagged to the CPT for loading [22], as shown in Fig. 3B.

The CPT release study from the DNA-NWs in the different media was conducted at physiological temperature (37 °C) and pH (7.45) to investigate the stability of CPT loading onto DNA-NWs for 5 h, as shown in Fig. 3C. The release of CPT was comparable to that of TE buffer (without serum) in the case of FBS as well as cell culture medium (with serum). In all three cases, the release of CPT was less than 75% after 6 h, indicating the stability of CPT loading onto DNA-NWs [37].

3.2. AFM and confocal characterization of DNA-NWs

DNA is a double-helical form that behaves differently in different designs of DNA nanotechnology structures. As a general rule, our designed DNA triangles were supposed to be arranged into DNA nano-sheets or nanoribbon lattices after self-assembly. However, as shown in the AFM images in Fig. 4A, two-dimensional DNA nano-sheets folded onto itself to give three-dimensional DNA-NWs due to the curvature of the DNA [38].

Confocal imaging of the DNA-NWs after loading with the FITC-tagged CPT is illustrated in Fig. 4B. We observed the effective CPT loading capability of the DNA-NWs. The AFM and confocal microscopic images revealed a uniform shape and size distribution of the DNA-NWs with lengths ranging from 2 to 4 μm and diameters ranging from 150 to 300 nm [24], shown in Figs. 4A and B.

3.3. Loading efficiency of CPT

UV absorption of CPT and DNA is close to each other at approximately 260−300 nm, making it challenging to analyze the CPT loading onto DNA-NW through UV spectrophotometry. To confirm CPT loading onto DNA-NWs, CPT was first conjugated with FITC using hook self-conjugating dyes (G-Biosciences, USA) with the purification columns available with the product. CPT has amino groups in its chemical structure, which is tagged with FITC by amide chemistry. Therefore, CPT loading was determined by UV analysis for the absorption of FITC in the range of 500−520 nm. After vacuum centrifugation at 14,000 rpm and 4 °C for 10 min of the CPT-loaded DNA-NWs, the unbound CPT in the supernatant

was removed. The CPT loading onto DNA-NW settled at the bottom and was measured using UV analysis [39]. The efficiency of CPT loading onto the DNA-NWs was calculated as 66.85%−97.35% for different concentrations of the CPT (0.1−51.2 nM) for various formulations (C1 to C10 respectively) (Table 2), keeping the DNA-NW concentration constant (20 μM). As a general trend, an increase in CPT concentration from the C1 to C10 formulations resulted in a decrease in the loading efficiency, keeping the DNA-NW concentration constant (30 μM). The loading efficiency was observed to be 97.35% in the case of 0.1 nM CPT (C1 formulation) to 66.85% in the
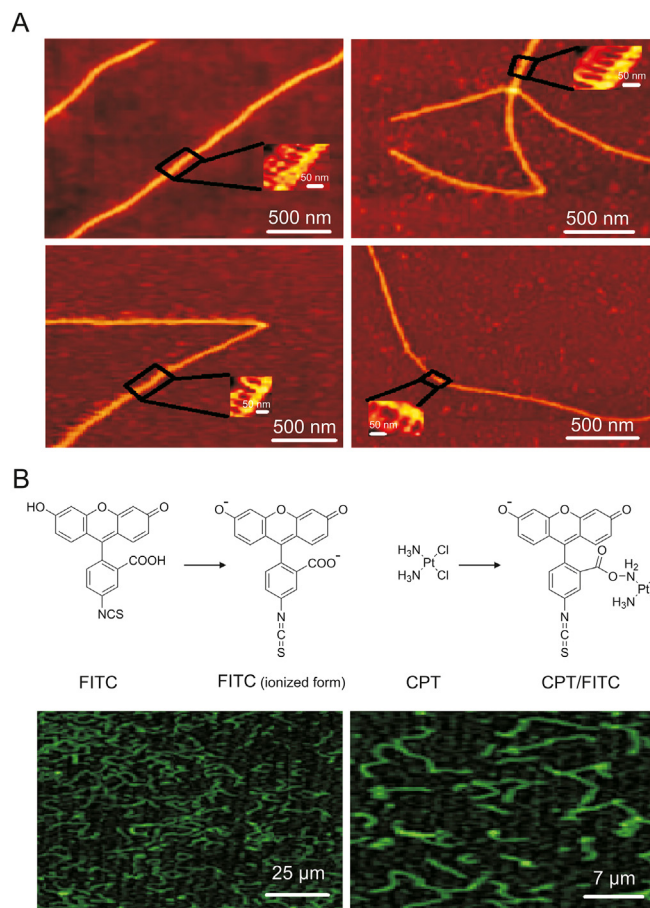
Fig. 4. AFM and confocal characterization of DNA-NWs. (A) AFM imaging of DNA-NWs. (B) Confocal imaging of FITC-tagged CPT-loaded DNA-NWs.

Table 2
CPT loading (%) of various formulations (C1-C10) with different concentrations of CPT.

Formulation	DNA-NW concentration (μM)	CPT concentration (nM)	Loading (%)
C1	20	0.1	97.35
C2	20	0.2	91.22
C3	20	0.4	86.16
C4	20	0.8	80.49
C5	20	1.6	77.33
C6	20	3.2	75.02
C7	20	6.4	73.71
C8	20	12.8	71.23
C9	20	25.6	68.34
C10	20	51.2	66.85

case of 51.2 nM (C10 formulation), at room temperature and physiological pH (pH 7.45). This finding might be due to the limited availability of binding sites and exposed pockets for CPT binding provided by consecutive G and C nucleotides, especially near the major and minor grooves of the double helix [19].

3.4. CPT docking simulation to bind with the DNA-NW

CPT is an inorganic drug that has excellent DNA-binding capability. We performed molecular docking of CPT binding with the DNA-NWs using autodock-vina/software from the template 3lpv.cif obtained from the protein-databank (https://www.rcsb.org/). Each CPT molecule can form two hydrogen bonds with either A, G, or C. However, the bond of CPT with C is stronger, with a bond length of 1.992 Å, as shown in Fig. 5. The bond length of CPT with the G was noted to be from 2.073 to 2.108 Å. CPT can bind to the DNA nanostructure at different positions, including its minor and major grooves. The cavities posed by the G and C nucleotides turned out to be the pockets for CPT deposition, as shown in Fig. 5. Hence, CPT

incubation with the DNA-NW resulted in effective loading onto DNA-NWs. Thus, CPT exhibited excellent affinity with the DNA-NW, as evidenced by the UV analysis [40,41], as shown in Fig. 3B.

3.5. Biocompatibility and cytotoxicity analysis of blank and CPT-loaded DNA-NW

The MTT test and flow cytometry were used to examine the biocompatibility and cytotoxicity of the blank DNA-NW and CPT-loaded DNA-NW. Various blank DNA-NW concentrations were applied to HepG2 cells for 24–48 h to observe cellular apoptosis. Using the MTT assay illustrated in Fig. 6A, the blank DNA-NW was biocompatible from a very low concentration of 10 μM to a very high concentration of 640 μM. However, the formulations with relatively high CPT (51.2 nM) contents (C10 formulation in Table 2) showed significantly higher cytotoxicity in a targeted manner than the free CPT solution. However, with the lower CPT concentrations, the cytotoxicity of the CPT-loaded DNA-NWs still significantly surpassed the free CPT solution. This finding might be due to decreased cell internalization of free CPT when used in lower concentrations (0.1-0.4 nM), resulting in slower first-order cell uptake of free CPT.

In the case of DNA-NWs loaded with CPT, polyanionic DNA-NWs showed better cell internalizations, even at extremely low concentrations, due to the binding of DNA-NWs with the scavenger receptors. It can be seen from the MTT results in Fig. 6B. The DNA-NW nanocarrier was efficient in terms of biocompatibility (Fig. 6A). It effectively enhanced CPT cytotoxicity at lower concentrations with an IC_{50} of 12.8 nM, compared with free CPT, exhibiting an IC_{50} of 51.2 nM (Fig. 6B). Similar findings were observed in the flow cytometry experiments shown in Fig. 6C. Empty DNA-NWs were highly biocompatible even at 640 μM, with 86% of the cells alive in the Q4 quadrant. These findings were similar to those of the blank solution (PBS), showing 89% of live cells. While CPT-loaded DNA-
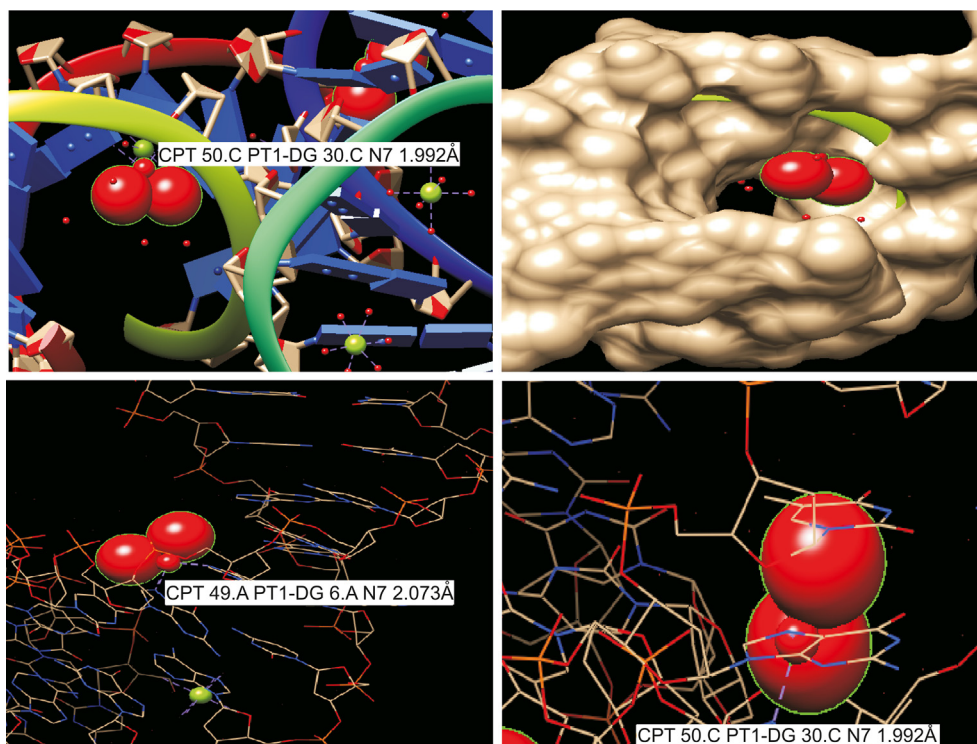
Fig. 5. CPT docking simulation to bind with the DNA-NW. Different bond lengths can be seen at different locations between the CPT and the DNA structure. The deposition of CPT in the DNA matrix is visible.

NW referring to formulation C7 with a CPT concentration of 6.4 nM caused late apoptosis in 22% of the cells in the Q2 quadrant. This finding suggests enhanced cytotoxicity in the case of CPT-loaded DNA-NWs compared with that of free CPT solution, as evident from the MTT assay results in Fig. 6B. However, late apoptotic effects might be due to the time required to internalize CPT-loaded DNA-NWs and its lysosomal digestion and sustained release of CPT in the cells. However, this technique might be useful for in vivo administration to avoid CPT's cytotoxic effects on healthy cells. Hence, DNA-NW is an efficient nanocarrier in terms of biocompatibility and enhances CPT's cytotoxicity, even at very low concentrations. DNA-NWs with nanoscale-sized structures large enough to load CPT effectively, and a dense and rigid nanomaterial, were used to load CPT in this study. In addition, dense DNA nanotechnology structures have been reported to be resistant to hydrolysis in body fluids, including blood and serum. Based on our in vitro evaluation, we believe that if applied in vivo, our DNA-NW design might have desired outcomes to target tumor cells without harming healthy cells [34].

3.6. Binding and internalization of DNA-NW in cells rich in scavenger receptors

DNA-NWs loaded with CPT (FITC-tagged) were applied to HepG2 cells that are rich in scavenger receptors. As a polyanionic drug carrier, DNA-NWs bind with the scavenger receptors on the cell surface, as illustrated in Fig. 7A. DNA-NWs were slowly internalized into cells with the time-dependent sustained or prolonged release of CPT within the cells, as evidenced by the gradual rise of green fluorescence of the FITC-tagged CPT on the cell surface after a 30 min interval as compared with the CHSE-214 cell line that lacks scavenger receptors. Hence, no internalization of DNA-NW was observed, as illustrated in Fig. 7B [9].

DNA-based nanomaterials are gaining importance as drug delivery carriers because of their precise nanoscale size and controlled shape. Some drugs such as dox and CPT have an intrinsic ability to bind with the DNA double helix, which can be effectively loaded onto DNA-based carriers. Furthermore, the polyanionic nature of DNA makes internalization by healthy cells difficult [4]. As cancer cells have a high proportion of polyanionic ligand-binding scavenger receptors, cancer cells can be effectively targeted [14]. DNA-NWs are nanoscale-sized, but big enough to load CPT effectively. DNA nanowires have a dense and rigid topology and are a suitable nanomaterial for CPT loading. Dense DNA nanotechnology structures are reported to be resistant to hydrolysis in body fluids, including blood and serum. Each triangle had 132 base pairs. One structural unit consists of 4 triangles containing 528 base pairs. Each nanowire has 10 to 25 structural units containing 5280 to 13,200 base pairs, with molecular weights of the DNA-NWs (polymer) of 1—4 million [42].
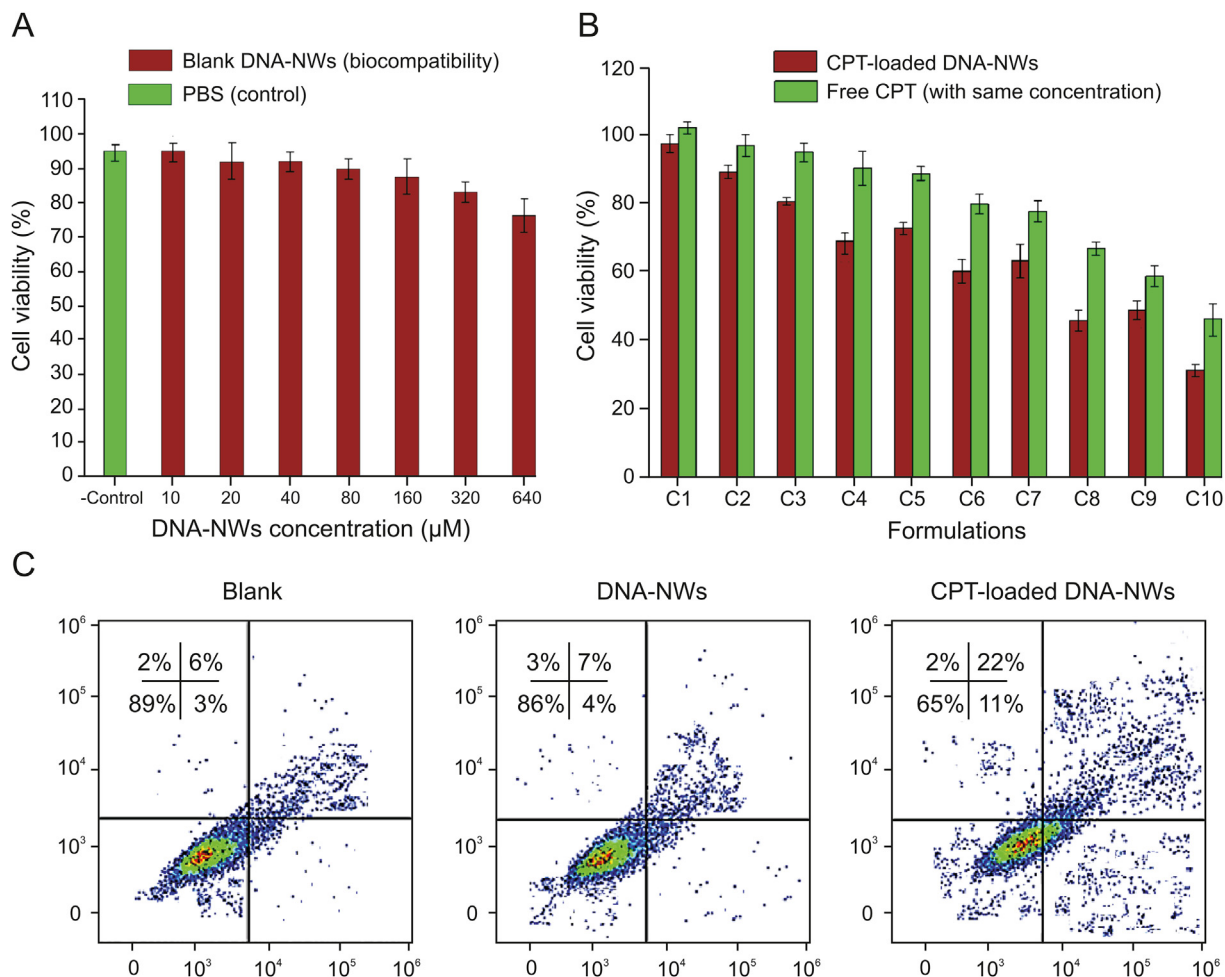
Fig. 6. Biocompatibility and cytotoxicity assay of blank and CPT-loaded DNA-NW. MTT assay of (A) biocompatibility of blank DNA-NWs and (B) cytotoxicity of CPT-loaded DNA-NWs compared with equivalent concentrations of free CPT solution. (C) Flow cytometry assessment of the biocompatibility of blank DNA-NW and the cytotoxicity of CPT-loaded DNA-NW.

A

HepG2 cells

B

CHSE-214 cells (control)
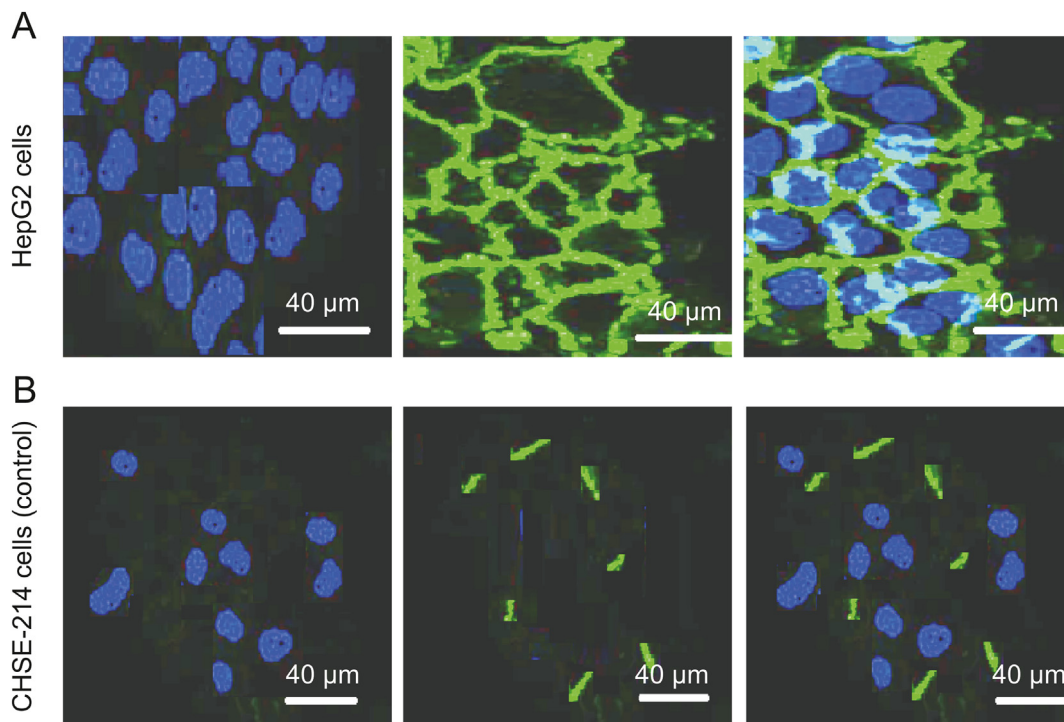
Fig. 7. Surface binding of DNA-NW loaded with FITC-tagged CPT to the human liver cancer cell line (HepG2) compared with the control cell line (CHSE-214) derived from the salmon embryo after a 30 min interval, scale bar = 40 μm. (A) As HepG2 cells are rich in scavenger receptors, DNA-NW binds the cell surfaces followed by gradual internalization into the cells and release of FITC-tagged CPT into the cytoplasm. (B) As CHSE-214 cells lack scavenger receptors, DNA-NW could not bind these cells, resulting in no cell internalizations.

4. Conclusions

Nano-architecture designed using a DNA-nanotechnology approach is receiving the attention of drug delivery scientists. This attention is due to the controllable nanoscale size, geometry, and drug loading and DNA-based vehicles' binding abilities. We designed DNA-NWs ranging in diameter from 150 to 300 nm and a length from 2 to 4 μm for loading CPT (loading efficiency 66.85%-97.35%) for anti-cancer resistance therapy. As many cancer cells, such as HepG2 cells, have large proportions of scavenger receptors that are polyanionic, they can be targeted using polyanionic drug delivery vehicles based on DNA nanomaterials. Being polyanionic nanocarriers for CPT, our DNA-NWs showed better cytotoxic effects and HepG2 cell internalization than the control cells (the CHSE-214 cell line). The apoptosis of the HepG2 cells with the CPT-loaded DNA-NWs was enhanced to 22% compared with the 7% apoptosis in the case of blank DNA-NWs. CPT-loaded DNA-NWs showed sustained release of CPT (75%) for 6 h in the presence or absence of serum (FBS) containing cell culture media is an evidence of its stability in serum-containing biological media. Hence, DNA-NWs turned out to be very effective nanocarrier in terms of biocompatibility and enhancing the cytotoxicity of CPT effectively at very low concentrations (IC_{50} of 12.8 nM) compared to the free CPT exhibiting an IC_{50} of 51.2 nM (see the results in Fig. 6). Based on our in vitro evaluation, if applied in vivo, our designed DNA-NWs might produce ideal outcomes in targeting tumor cells without harming healthy cells.

Declaration of competing interest

The authors declare that there are no conflicts of interest.

Acknowledgments

References

[1] G.J. Khan, M. Rizwan, M. Abbas, et al., Pharmacological effects and potential therapeutic targets of DT-13, Biomed. Pharmacother. 97 (2018) 255—263.
[2] W. Wang, M. Naveed, M.M.F.A. Baig, et al., Experimental rodent models of chronic prostatitis and evaluation criteria, Biomed, Pharma 108 (2018) 1894—1901.
[3] V. Morello, S. Cabodi, S. Sigismund, et al., B1 integrin controls EGFR signaling and tumorigenic properties of lung cancer cells, Oncogene 30 (2011) 4087—4096.
[4] Y.X. Zhao, A. Shaw, X. Zeng, et al., DNA origami delivery system for cancer therapy with tunable release properties, ACS Nano 6 (2012) 8684—8691.
[5] W. Witt, I. Kolleck, H. Fechner, et al., Regulation by vitamin E of the scavenger receptor BI in rat liver and HepG2 cells, J. Lipid Res. 41 (2000) 2009—2016.
[6] M.M.F.A. Baig, Q.-W. Zhang, M.R. Younis, et al., A DNA nano-device simultaneously activating the EGFR and integrin for enhancing cytoskeletal activity and cancer cell treatment, Nano Lett. 19 (2019) 7503—7513.
[7] M. Naveed, L. Phil, M. Sohail, et al., Chitosan oligosaccharide (COS): an overview, Int. J. Biol. Macromol. 129 (2019) 827—843.
[8] M.Y. Ben Zion, X. He, C.C. Maass, et al., Self-assembled three-dimensional chiral colloidal architecture, Science 358 (2017) 633—636.
[9] Q. Jiang, C. Song, J. Nangreave, et al., DNA origami as a carrier for circumvention of drug resistance, J. Am. Chem. Soc. 134 (2012) 13396—13403.
[10] M. Abbas, M.M.F.A. Baig, Y. Zhang, et al., A DNA-based nanocarrier for efficient cancer therapy, J. Pharm. Anal. (2020), https://doi.org/10.1016/j.jpha.2020.03.005.
[11] Q. Zhang, Q. Jiang, N. Li, et al., DNA origami as an in vivo drug delivery vehicle for cancer therapy, ACS Nano 8 (2014) 6633—6643.
[12] M.M.F.A. Baig, W.-F. Lai, A. Ahsan, et al., Synthesis of ligand functionalized ErbB-3 targeted novel DNA nano-threads loaded with the low dose of

doxorubicin for efficient in vitro evaluation of the resistant anti-cancer activity, Pharm. Res. 37 (2020) 75.

[13] P.D. Halley, C.R. Lucas, E.M. McWilliams, et al., Daunorubicin-loaded DNA origami nanostructures circumvent drug-resistance mechanisms in a leukemia model, Small 12 (2016) 308—320.

[14] M.M. Thi, S.O. Suadicani, M.B. Schaffler, et al., Mechanosensory responses of osteocytes to physiological forces occur along processes and not cell body and require V 3 integrin, Proc. Natl. Acad. Sci. Unit. States Am. 110 (2013) 21012—21017.

[15] R.A. Brady, N.J. Brooks, V. Foderà, et al., Amphiphilic-DNA platform for the design of crystalline frameworks with programmable structure and functionality, J. Am. Chem. Soc. 140 (2018) 15384—15392.

[16] M.M.F.A. Baig, S. Khan, M.A. Naeem, et al., Vildagliptin loaded triangular DNA nanospheres coated with eudragit for oral delivery and better glycemic control in type 2 diabetes mellitus, Biomed. Pharmacother. 97 (2018) 1250—1258.

[17] X. Shi, W. Lu, Z. Wang, et al., Programmable DNA tile self-assembly using a hierarchical sub-tile strategy, Nanotechnology 25 (2014), 075602.

[18] S.H. Park, R. Barish, H. Li, et al., Three-helix bundle DNA tiles self-assemble into 2D lattice or 1D templates for silver nanowires, Nano Lett. 5 (2005) 693—696.

[19] M.M.F.A. Baig, M. Sohail, A.A. Mirjat, et al., PLL-alginate and the HPMC-EC hybrid coating over the 3D DNA nanocubes as compact nanoparticles for oral administration, Appl. Nanosci. 9 (2019) 2105—2115.

[20] S. Lopez-Gomollon, F.E. Nicolas, Purification of DNA oligos by denaturing polyacrylamide gel electrophoresis (PAGE), Methods Enzymol. 529 (2013) 65—83.

[21] M.M.F.A. Baig, M. Naveed, M. Abbas, et al., DNA scaffold nanoparticles coated with HPMC/EC for oral delivery, Int. J. Pharm. 562 (2019) 321—332.

[22] M.M.F.A. Baig, M. Abbas, M. Naveed, et al., Design, synthesis and evaluation of DNA nano-cubes as a core material protected by the alginate coating for oral administration of anti-diabetic drug, J. Food Drug Anal. 27 (2019) 805—814.

[23] N. Afshan, M. Ali, M. Wang, et al., DNA nanotubes assembled from tensegrity triangle tiles with circular DNA scaffolds, Nanoscale 9 (2017) 17181—17185.

[24] M. Li, H. Zuo, J. Yu, et al., One DNA strand homo-polymerizes into defined nanostructures, Nanoscale 9 (2017) 10601—10605.

[25] P. O'Neill, P.W.K. Rothemund, A. Kumar, et al., Sturdier DNA nanotubes via ligation, Nano Lett. 6 (2006) 1379—1383.

[26] M.M.F. A Baig, W.-F. Lai, R. Mikrani, et al., Synthetic NRG-1 functionalized DNA nanospindels towards HER2/neu targets for in vitro anti-cancer activity assessment against breast cancer MCF-7 cells, J. Pharmaceut. Biomed. Anal. 182 (2020), 113133.

[27] R. Peng, X. Zheng, Y. Lyu, et al., Engineering a 3D DNA-logic gate nanomachine for bispecific recognition and computing on target cell surfaces, J. Am. Chem. Soc. 140 (2018) 9793—9796.

[28] Z. Liu, C. Tian, J. Yu, et al., Self-assembly of responsive multilayered DNA nanocages, J. Am. Chem. Soc. 137 (2015) 1730—1733.

[29] M.M.F.A. Baig, M. Naveed, M. Abbas, et al., Chitosan-coated rectangular DNA nanospheres for better outcomes of anti-diabetic drug, J. Nanoparticle Res. 21 (2019), 98.

[30] R. Hajian, P. Hossaini, Z. Mehrayin, et al., DNA-binding studies of valrubicin as a chemotherapy drug using spectroscopy and electrochemical techniques, J. Pharm. Anal. 7 (2017) 176—180.

[31] A. Mann, R. Richa, M. Ganguli, DNA condensation by poly-l-lysine at the single molecule level: role of DNA concentration and polymer length, J. Contr. Release 125 (2008) 252—262.

[32] Y. Zhang, R. Zhang, X. Yang, et al., Recent advances in electrogenerated chemiluminescence biosensing methods for pharmaceuticals, J. Pharm. Anal. 9 (2019) 9—19.

[33] M.M.F.A. Baig, X.-H. Xia, The PA-receptor mediated internalization of carboplatin loaded poly-anionic DNA-nanowires for effective treatment of resistant hepatic-cancer HepG-2 cells, Appl. Nanosci. 10 (2020) 1915—1926.

[34] D. Agudelo, P. Bourassa, G. Bérubé, et al., Intercalation of antitumor drug doxorubicin and its analogue by DNA duplex: structural features and biological implications, Int. J. Biol. Macromol. 66 (2014) 144—150.

[35] M. Zayed, C. Tourne-Peteilh, M. Ramonda, et al., Microgels of silylated HPMC as a multimodal system for drug co-encapsulation, Int. J. Pharm. 532 (2017) 790—801.

[36] R. Hajian, Z. Tayebi, N. Shams, Fabrication of an electrochemical sensor for determination of doxorubicin in human plasma and its interaction with DNA, J. Pharm. Anal. 7 (2017) 27—33.

[37] N. Seedat, R.S. Kalhapure, C. Mocktar, et al., Co-encapsulation of multi-lipids and polymers enhances the performance of vancomycin in lipid-polymer hybrid nanoparticles: in vitro and in silico studies, Mater. Sci. Eng. C 61 (2016) 616—630.

[38] M.M. Ali, F. Li, Z. Zhang, et al., Rolling circle amplification: a versatile tool for chemical biology, materials science and medicine, Chem. Soc. Rev. 43 (2014) 3324—3341.

[39] Y. Nakayama, H. Yamaguchi, N. Einaga, et al., Pitfalls of DNA quantification using dnabinding fluorescent dyes and suggested solutions, PloS One 11 (2016), e0150528.

[40] X. Wang, D.Y. Huang, S.M. Huong, et al., Integrin αvβ3 is a coreceptor for human cytomegalovirus, Nat. Med. 11 (2005) 515—521.

[41] M.M.F.A. Baig, M. Naveed, M. Abbas, et al., Evaluation of chitosan/eudragit hybrid coating over cubic DNA nanospheres with superior stability and therapeutic outcomes, J. Drug Deliv. Sci. Technol. 52 (2019) 577—585.

[42] W. Wang, S. Chen, B. An, et al., Complex wireframe DNA nanostructures from simple building blocks, Nat. Commun. 10 (2019), 1067.